Geomorphology 323 (2018) 98–105

Contents lists available at ScienceDirect

Geomorphology

journal homepage: www.elsevier.com/locate/geomorph

Flume experiments on flow and sediment supply controls on gravel bedform dynamics

Peter A. Nelson*, Jacob A. Morgan

Department of Civil and Environmental Engineering, Colorado State University, 1372 Campus Delivery, Fort Collins, CO 80523-1372, USA

ARTICLE INFO

Article history:
Received 23 December 2017
Received in revised form 9 September 2018
Accepted 9 September 2018
Available online 18 September 2018

Keywords:
Gravel bedforms
Alternate bars
Sediment supply
Unsteady flow
Flume experiment

ABSTRACT

We present results from a flume experiment in which we investigate how the formation and dynamics of gravel bedforms are affected by changes in discharge and sediment supply. We conducted experiments in a straight rectangular sediment feed flume using a unimodal mixture of fine gravel and coarse sand. The experiment consisted of three phases: (1) equilibrium sediment supply and steady flow, (2) equilibrium sediment supply and repeated hydrographs, and (3) doubled sediment supply and repeated hydrographs. During the experiments, low-amplitude, migrating bedforms resembling alternate bars developed and their dynamics were characterized and tracked via collection of repeated structure-from-motion topographic data sets. Channel-scale morphology was essentially the same for steady and unsteady flow at the same sediment supply, but the bedform celerity was much lower with unsteady flow than it was under constant discharge. Bedform amplitudes increased on the rising limb of the hydrograph and declined on the falling limb, but their wavelength was largely insensitive to flow variation. When the sediment supply was increased, the dominant channel response was an increase in slope. The bedform celerity increased, but not to the same rate as under steady flow. Although our experiment developed alternate bars, the width-to-depth ratio of 8 indicates that present theory would not predict the occurrence of bars for our conditions. Our observations show that alternate bars may develop under low width-to-depth conditions and suggest that further theoretical development is needed to identify the mechanism responsible for their formation.

1. Introduction

Heterogeneous, coarse-grained riverbeds often self-organize into migrating or stationary bedforms such as pebble clusters (e.g., Brayshaw et al., 1983), bedload sheets (Whiting et al., 1988; Nelson et al., 2009), gravel dunes (Carling, 1999), and alternate bars (e.g., Venditti et al., 2012; Nelson et al., 2014; Bankert and Nelson, 2017). These features can be important sources of flow resistance, they can have a significant influence on the temporal variability of sediment transport rates, and in the case of bars, they may be responsible in part for the development of meanders and channel migration (e.g., Blondeaux and Seminara, 1985).

Sediment supply is increasingly acknowledged to play an important role in the formation and dynamics of bedforms in gravel-bed rivers. Venditti et al. (2017) suggested that sediment supply and the relative mobility of the bed surface sediment affect the type of bedforms that may be present in gravel-bed rivers; and they developed a conceptual gravel bedform phase diagram where sediment supply is a primary control, while flow strength plays a secondary role in the types of bed features that emerge. Sediment supply has also been shown to control the dynamics of bedload sheets, which are downstream-migrating sorting features with fine tails and coarse fronts 1–2 grain diameters high. Under high sediment supply, bedload sheets move faster and are more closely spaced than they are under lower supply conditions (Nelson et al., 2009). Alternate bars have been shown to disappear when sediment supply is eliminated (Venditti et al., 2012) and to develop into short-wavelength transient features when sediment supply is increased (Podolak and Wilcock, 2013; Bankert and Nelson, 2017). Sediment supply also has been correlated with the depth of sediment in pools (Lisle and Hilton, 1992) and with the stability of step-pool features (Recking et al., 2012).

Despite the recent efforts directed toward better understanding the importance of sediment supply on gravel bedforms, we still have a rather limited understanding of how changes in sediment supply may become manifest through the occurrence of different bedform types, changes in bedform dynamics (i.e., bedform geometry and migration characteristics), overall changes in channel slope or bed surface sorting, or some combination of all of these. This is

* Corresponding author.
E-mail address: peter.nelson@colostate.edu (P.A. Nelson).

https://doi.org/10.1016/j.geomorph.2018.09.011
0169-555X/

largely because the conditions in gravel-bed rivers are frequently in a state of partial or selective transport, where the coarser fractions of the bed surface grain-size distribution are either not transported as bedload or they are transported at a proportion smaller than their representation on the bed surface (Parker, 2008). The dynamic relationship between sediment supply and bed surface composition and patchiness (e.g., Dietrich et al., 1989; Nelson et al., 2009) potentially complicates our understanding of gravel bedform dynamics under different sediment supplies.

The effects of unsteady flow on gravel bedform dynamics are also not well understood. Gravel-bed rivers often show hysteresis in bedload transport, potentially caused by different sediment availability conditions between the rising and falling limbs of a hydrograph (Hassan and Church, 2001) or to changes in bed structure during the hydrograph (Mao, 2012). Sand-bed flume experiments on alternate bar formation under unsteady flow found that bar celerities increased on the rising limb of the hydrograph and fell on the falling limb of the hydrograph and that bar development is strongly controlled by nonlinear effects and flow unsteadiness (Tubino, 1991a). However, the effects of unsteady flow conditions on gravel bar dynamics, which may be subject to hysteresis in sediment transport rates and partial or selective transport, are unclear.

Here, we seek greater insight on the influence of sediment supply and unsteady flow on gravel bedform dynamics. To that end, we have conducted a flume experiment in which we imposed steady and unsteady flow with two different sediment supplies and documented in detail the morphodynamic evolution of the channel and the dynamics of the bedforms that developed. Our results suggest that unsteady flow has a negligible impact on channel-scale morphology, but is an important control on gravel bedform characteristics and dynamics, and that increasing sediment supply slightly modifies bedform dynamics but dramatically increases the overall channel slope. Our observations also provide evidence of alternate bars in low width-to-depth ratio conditions, raising important questions about linear theories of alternate bar formation.

2. Methods

2.1. Flume configuration

Flume experiments were conducted at the hydraulics laboratory at the Colorado State University Engineering Research Center, as part of a larger study aimed at understanding how flow, sediment supply, and channel width variation affect the dynamics of riffle-pool sequences. In this study, flume experiments were conducted in a straight-walled channel and in a variable-width channel, but in this paper we focus on observations of bedforms collected during experiments conducted in the straight-walled channel only. A description of the full suite of experiments using both constant- and variable-width flume geometries is provided in Morgan (2018).

The experiment was conducted in a 0.87-m-wide, 18-m-long, straight-walled rectangular flume. The initial bed slope, discharge, and grain-size distribution were chosen so that (i) the width-to-depth ratio in the wide sections of the variable-width channel would be about 15, which is representative of the fairly wide, shallow flow characteristic of riffles (Richards, 1976; Milan, 2013), and (ii) all grain sizes in the distribution would be mobile and transported primarily as bedload. The sediment composing the initial bed surface and the sediment feed mixture used throughout the experiments was a unimodal mixture of primarily fine gravel with a small proportion of coarse sand (Fig. 1), ranging in size from 0.5 to 8 mm, with a median diameter (D_{50}) of 3.4 mm. The flume experiment was performed to investigate mechanisms of morphodynamic response and was not designed to model any particular prototype river; however, if we use the scaling relationship of Parker et al. (2003) and riffle width measurements reported by Carling and Orr (2000) and Brew et al. (2015), the model sediment scales up to a gravel distribution ranging from 20 to 320 mm, with a median of 136 mm. The initial bed was screeded flat and set to a slope of 0.007, which is characteristic of natural gravel-bed rivers with alternate bars or riffle-pool morphology (e.g., Montgomery and Buffington, 1997).

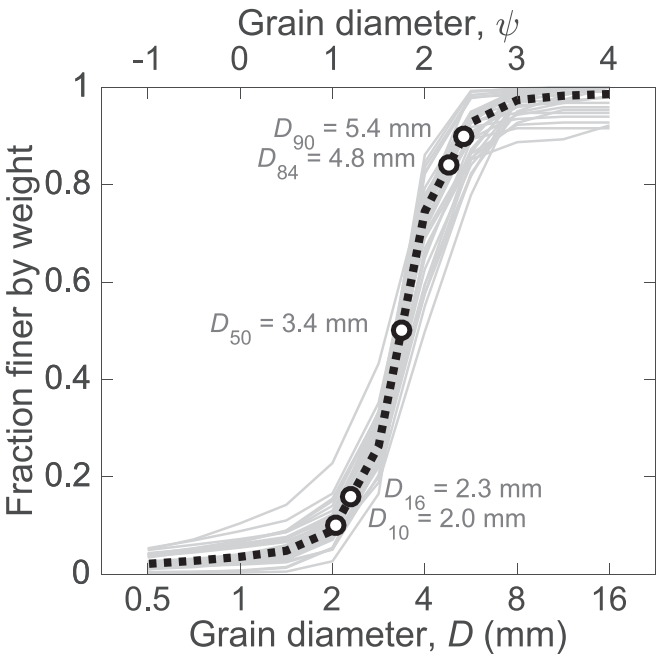

Fig. 1. Volume-by-weight grain-size distribution of the bulk sediment mixture. Gray curves are grain-size distributions of individual samples; the dashed black line is the average.

The experiment was set up in three phases. In phase 1 (denoted F01P01 in subsequent figures), we imposed a constant water discharge and constant sediment supply. In phase 2 (F01P02), the sediment supply was unchanged, but instead of constant water discharge we imposed a repeated triangular hydrograph. In phase 3 (F01P03), we continued to use the same repeated hydrograph as in phase 2 but doubled the sediment supply rate. The three phases were continuous; i.e., the bed was not rescreeded flat between phases. Using this experimental design, our intent was to be able to isolate the influence of constant vs. variable discharge (phase 1 vs. phase 2) and to isolate the influence of changing sediment supply (phase 2 vs. phase 3) on the morphodynamic evolution of the channel.

The initial, constant, discharge used in phase 1 was set to 58.3 L/s. Given our initial slope and grain-size distribution, we determined that this discharge would result in an average dimensionless boundary shear stress ($\tau^* = \tau/(\rho_s - \rho)gD_{50}$, where τ is the boundary shear stress, ρ_s and ρ are the densities of sediment and water, and g is gravitational acceleration) ~2 times the critical value for the median grain size, assumed here to be about $\tau_c^* = 0.045$, as we expected that excess shear stress to be able to mobilize the entire grain-size distribution (Wilcock and McArdell, 1993). The downstream water surface elevation was controlled by an adjustable tailgate, which was set to a level that produced normal flow conditions of constant depth and water surface slope for at least the last 2 or 3 m at the downstream end of the flume.

The repeat hydrographs imposed during phases 2 and 3 had a triangular shape, with an average value equal to the steady flow discharge used in phase 1 (58.3 L/s), a minimum of 49.2 L/s, and a maximum of 67.4 L/s. Individual hydrographs had a period of 120 min, which using the Parker et al. (2003) scaling mentioned above corresponds to a duration of about 13 h in the field, and the hydrographs were stepped such that the flow was increased or decreased by an

increment of ~3 L/s every 10 min. We chose a symmetric triangular hydrograph to keep the shape as simple as possible. The peak discharge was dictated by the maximum flow the water supply pipe our experiments were using could accommodate, and the minimum flow was set so that the mean discharge equaled that used during the steady flow experiments of phase 1.

During all three phases, the bulk sediment mixture (Fig. 1) was fed into the channel at the upstream end using a sediment feeder consisting of a large hopper connected to a horizontal enclosed auger controlled by a variable-speed motor. Prior to the experiment, a rating curve relating the motor speed to the sediment feed rate was developed, and this relationship was used to control the sediment supply rate during the experiments. The sediment was fed at a constant rate during all three phases. The feed rate in phase 1 and 2 was 1580 g/min, which was selected by calculating the expected average boundary shear stress for our initial slope, water discharge, and grain-size distribution and by using the Wilcock and Crowe (2003) relation to estimate the equilibrium sediment transport rate. The feed rate in phase 3 was twice that of phases 1 and 2 (3160 g/min).

Sediment exiting the flume as bedload was collected in a sediment trap. When the trap became filled with sediment (approximately every 3 h during phases 1 and 2 and more frequently during the high-supply phase 3), the experiment was halted by shutting down the water pumps and sediment feeder. Care was taken to ensure that bed adjustments caused by stopping and restarting the flow were minimized, and we did not visually observe any bed disturbance associated with these experimental breaks. During these periods, the sediment was removed from the trap, and samples of it were dried, sieved, and weighed to determine the rate of sediment exiting the channel and the size distribution of the transported sediment.

The flume was equipped with a computer-controlled instrumentation cart that traversed the length of the flume along rails mounted to the flume walls. Water surface elevation during the experiments was measured by five ultrasonic water level sensors mounted to the cart, spaced 11 cm apart. These sensors produced five simultaneous longitudinal water surface profiles as the cart moved along the channel. Measurements in the along-channel direction were obtained at intervals of 5–10 cm, and water surface scans were conducted continuously throughout the experiment. Each water surface scan took ~ 3–8 min to complete.

Each time the flume was shut down, the bed was allowed to drain, and a series of photographs were collected to characterize bed topography using structure-from-motion (SfM) photogrammetry. Morgan et al. (2017) demonstrated that SfM techniques in the laboratory can achieve accuracy and resolution as good or better than terrestrial laser scanners. Photos were taken with an 18-megapixel Canon EOS Rebel T3i with an 18–55 mm IS II lens. The camera was mounted to the cart and oriented ~45° below horizontal. Images were first collected in the upstream and downstream directions, with the focal length set to 18 mm and a longitudinal spacing of about 0.28 m, producing about 120 photos. Images were then collected with the camera facing in the downstream direction, with the focal length set to 55 mm and a longitudinal spacing of 0.17 m, producing about 100 photos. The resulting photo data sets therefore consisted of 220 photos with substantial (≥80%) overlap between adjacent images. Targets with known position were mounted to the flume walls and captured in the images along with the flume bed; these were identified during SfM analysis and used to scale and register the topographic data sets. The photo sets were imported into Agisoft PhotoScan Professional for SfM analysis, producing point clouds usually consisting of about 400 million topographic data points. These point clouds were then interpolated onto a 0.5-mm grid using the natural neighbor algorithm, and we use these topographic grids in our analysis in this paper. The grids analyzed in this paper cover the full 0.87-m width of the channel and show longitudinal coordinates from 4.5 m downstream of the flume headbox to 17.5 m downstream (i.e., 0.5 m from the outlet). From our analyses of these digital elevation models, in addition to the work of Morgan et al. (2017) conducted in the same flume, we estimate the vertical uncertainty of the elevation data to be on the order of about 1 mm.

Although SfM data sets were typically collected just when the sediment trap became full (every 2–3 h), we also drained the flume and collected SfM data at higher temporal resolution for portions of each phase so that the topographic data could be used to characterize the dynamics of the bedforms that developed. During the steady-flow conditions of phase 1, high-resolution scans were taken over a 120-min period, with scans every 15 min, while during phases 2 and 3 the flume was drained and photo sets collected each time the hydrograph was stepped (every 10 min) for two complete hydrographs (a 240-min period).

Each phase of the experiment was run until we were confident that steady-state conditions had been reached, indicated by essentially unchanging rates and grain sizes of sediment exiting the flume and unchanging bed and water surface slopes computed from the SfM and ultrasonic water level sensor data respectively. Ultimately, phase 1 had a duration of 4154 min (69.2 h), phase 2 had a duration of 3000 min (50 h), and phase 3 had a duration of 2280 min (38 h).

2.2. Bedform characteristics

The 0.5-mm topographic grids were used to characterize the wavelength, amplitude, and celerity of bedforms that developed during the experiments. We adopted an approach similar to that taken by van der Mark et al. (2008), Martin and Jerolmack (2013), and others. The bedforms in our experiments were predominately located on alternate sides of the channel, so we characterized them by averaging the elevation of the left and right 15 cm of each cross section in the grid, and we subtracted the right-side average elevation from the left-side average elevation for each cross section (Fig. 2). We then found the locations at which this profile of elevation differences crossed the zero line (zero crossings), and then defined the tops of the bedforms to be the local maxima and minima between zero crossings. The downstream distance between consecutive maxima or consecutive minima then defines the wavelength of each bedform, and the elevation difference between adjacent bar tops (i.e., maximum-minimum pairs) defines the bedform amplitude (Fig. 2).

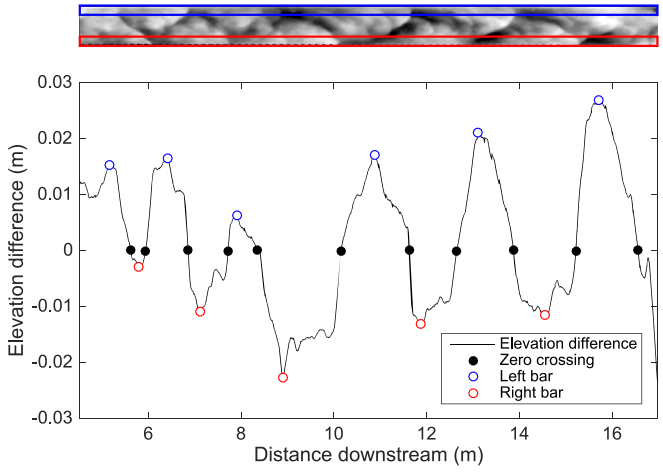

Fig. 2. Example showing calculation of bar wavelengths and amplitudes. Average elevations of the left and right sides of the channel (within the blue and red areas in the detrended topography map) were differenced. Zero-crossings of the difference were identified, and local minimum and maximum elevations between zero-crossing locations identify bar crests.

Bedform celerities were computed in a similar manner for the periods for which we have high-temporal-resolution topographic data sets. For each topographic grid, longitudinal profiles of the left and right sides of the channel were visually compared to profiles from the topographic grid from the subsequent scan. The locations of bedforms that could be readily identified in each grid were then recorded, ultimately producing a space-time data set of bedform migration (Fig. 3). The lines in Fig. 3 represent the motion of individual bedforms, so the slopes of the lines allow us to determine the migration rates of each bedform.

3. Results

3.1. Flume-average conditions

Fig. 4 presents a summary of the flow conditions and sediment transport characteristics throughout all three phases of the experiment. During phase 1, bedload initially exited the flume at a much higher rate than the sediment feed rate, but within about 20 h of run time the outgoing bedload flux and the sediment flux had equilibrated. During this initial period, the bed slope reduced from the initial 0.7% to 0.44%, where it remained for the rest of phase 1. The grain size of the material exiting the flume was basically unchanging throughout phase 1, with a D_{50} of about 3.3 mm. The average water depth during phase 1 was 11 cm, resulting in a width-to-depth ratio (β) of 8. The Froude number ($Fr = U/\sqrt{gh}$, where U is the average velocity, g is gravitational acceleration, and h is the average depth) was about 0.6 during phase 1.

No significant changes to flume-averaged hydraulic and bed characteristics occurred after the repeated hydrograph was introduced during phase 2 (Fig. 4), although bedform characteristics did undergo changes as discussed in the following section. The bed and water surface slopes were about 0.42% and 0.5% respectively throughout phase 2, and the exiting bedload D_{50} remained about 3.2 mm. The average flow depth was 11 cm, the width-to-depth ratio was 8, and the Froude number was 0.6.

More substantial flume-averaged changes occurred during phase 3 when the sediment feed rate was doubled. The bedload exiting the flume responded to the feed increase quickly, as the average transport rate from the first sample collected a few hours after the phase began was approximately the same as the new feed rate (Fig. 4). The D_{50} of the bedload exiting the flume increased slightly for about 10 h, then relaxed back to the D_{50} of the feed mixture. Average flow depths decreased slightly to 10 cm, increasing the width-to-depth ratio to about 8.5, and the Froude number increased slightly to about 0.65. The primary change that occurred during phase 3 was an increase in the bed and water surface slopes to about 0.55% and 0.62% respectively.

3.2. Bedform characteristics

Migrating bedforms were observed during all three phases of the experiment. The bedforms tended to occupy alternating sides of the channel in the downstream direction and exhibited lobate fronts. These features are evident in the photo of the flume shown in Fig. 5,

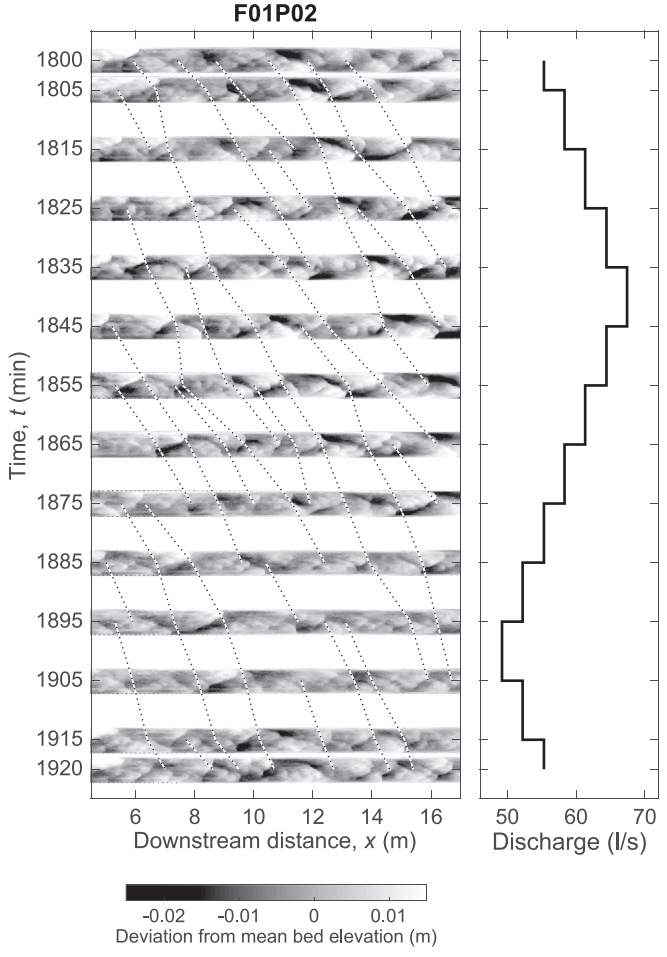

Fig. 3. Detrended topographic maps of the flume bed over the course of a hydrograph (F01P02), showing manually identified bedform crest positions used to compute bedform celerities.

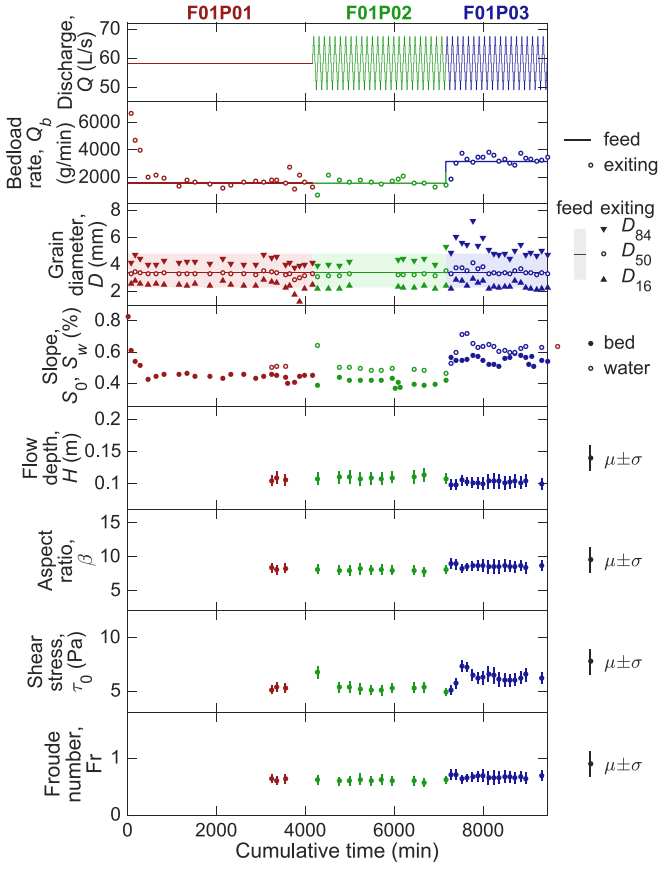

Fig. 4. Time series of hydraulic conditions and sediment transport characteristics during all three phases of the experiment.

Fig. 5. Photograph of the flume as it was draining, illustrating the alternate bars that developed. View is looking downstream.

as well as the data shown in Figs.2 and 3. Because these are classical characteristics of alternate bars, we will refer to these bedforms as *bars* for the rest of this paper.

The wavelength, amplitude, and celerity of the alternate bars during the three high-temporal-resolution scanning periods of each experimental phase are presented in Fig. 6. The average wavelength of the bars was consistently around 2 to 2.5 m during all three phases, although individual bar wavelengths could range from under 1 to over 6 m. The average amplitude of the bars also remained constant at around 3 cm throughout all three phases; however, during phases 2 and 3, the average bar amplitude tended to track with the discharge, suggesting that increasing and decreasing flow depths caused the bar amplitudes to also increase and decrease. The average celerity of the bars during phase 1 was about 0.3 m/min. When the flow transitioned to repeat hydrographs during phase 2, the average bar celerity decreased to about 0.1 m/min, and doubling the sediment supply while maintaining the same repeat hydrographs in phase 3 resulted in average bar celerity of about 0.17 m/min.

4. Discussion

4.1. Flow and sediment supply controls on gravel bedform dynamics

The three phases of our experiment allow us to investigate how unsteady flow and changes in sediment supply affect gravel-bed morphodynamics and the characteristics of migrating alternate bars.

First, the transition in our experiment from steady flow to repeated hydrographs had almost no effect on the overall characteristics of the channel. This finding is in general agreement with previous gravel-bed flume experiments with unsteady flow (but without freely formed alternate bars) (e.g., Wong and Parker, 2006; Humphries et al., 2012; Mao, 2012), which have found that the shape and duration of the hydrograph generally does not have a strong influence on parameters such as slope, surface grain size, and sediment transport rate. This is likely because the timescale of flow variability (i.e., the duration of the hydrograph) is generally much shorter than the timescale for morphodynamic adjustment, so the

local sediment transport rate adjusts to changes in discharge rapidly, thereby preventing excessive erosion or deposition. Flume and modeling studies by Wong and Parker (2006) and Parker et al. (2008) have proposed that for conditions where the flow is unsteady but the sediment supply is constant, a so-called 'hydrograph boundary layer' develops wherein bed-surface adjustments only occur over a short upstream portion of the channel, while for the majority of the channel the bed elevation and surface size distribution are invariant to the changing flow because the bedload transport rate and grain size absorb nearly all of the variation in the flow.

The increased sediment supply from phase 2 to phase 3, however, produced significant flume-scale changes, primarily via an increase in the bed and water surface slope. Gravel-bed channels can adjust to changing sediment supply through surface grain size adjustment or by changing their slope (e.g., Lane, 1955). Decreases in sediment supply lead to overall bed coarsening as patches of coarse sediment expand and patches of fine sediment shrink (Dietrich et al., 1989; Nelson et al., 2009), but in our experiment the bed during phases 1 and 2 did not display obvious sorting patterns or bed armoring, suggesting that the sediment feed rate approximated the transport capacity of the channel. When the sediment supply was increased in phase 3, the bed could not get any finer, leaving overall slope change as the only option.

The decrease in bar celerity from phase 1 to phase 2 (Fig. 6), when the water discharge transitioned from steady flow to repeat hydrographs, is striking; and the reason the bar migration rate decreased so much in response to the unsteady flow is not clear. Previous studies documenting migrating alternate bars have generally found that the migration rate tends to increase with increasing discharge or boundary shear stress; for instance, Lanzoni (2000a,b) found that bar celerity generally increased with bed slope and sediment transport rate under steady flow, and Tubino (1991b) found that under unsteady flow the celerity of bars increased on the rising limb and fell during the falling limb. Tubino (1991b) also pointed out, however, that unsteady flow has two counteracting effects on bar celerity: increasing discharge increases bar celerity, but finite amplitude effects damp bar celerity as the bar amplitude increases.

We speculate that the decreased bar celerity under unsteady flow conditions we observed in our experiments may be a consequence of the nonlinear relationship between bed stress and sediment transport rates. The portions of the hydrograph with discharge lower than the steady discharge of phase 1 may have experienced much lower sediment transport rates and therefore bar migration rates; and during the portions of the hydrograph where the flow exceeded the steady flow of phase 1 the increase in sediment transport rate, relative to phase 1, may have gone into building up the bar amplitude rather than increasing the bar celerity. Indeed, Fig. 6 shows that although celerities were lower in phases 2 and 3 than they were in phase 1, the bar amplitudes during the high-flow portions of the hydrographs tended to be larger than bar amplitudes during phase 1.

4.2. Connecting observations to theory

The bedforms that developed during our experiments display the classical characteristics of alluvial alternate bars: they occur on alternating sides of the channel, they display lobate fronts, their wavelengths do not vary with changes in depth (bar wavelengths

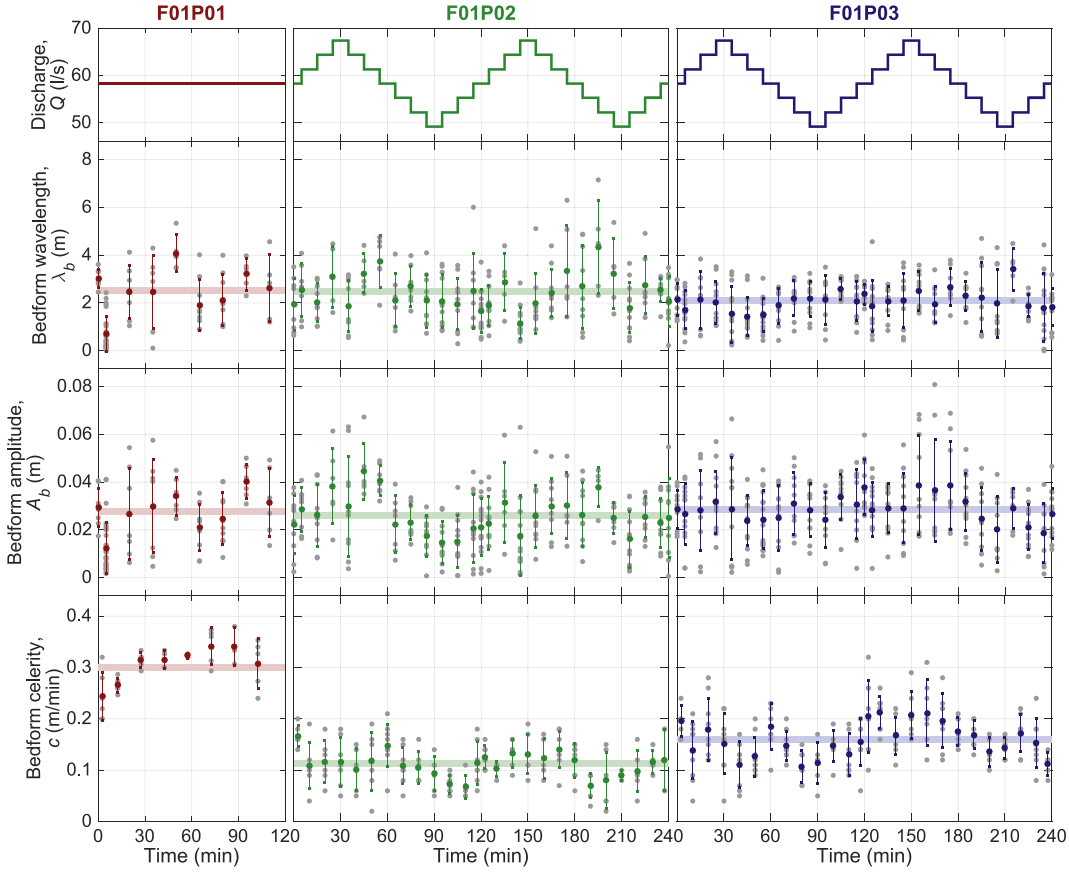

Fig. 6. Bedform wavelength, amplitude, and celerity during individual hydrographs for the three phases of the experiment (time series are not continuous from one phase to the next).

are generally thought to scale with channel width, which in our experiments was constant), but their amplitude did increase with increasing flow depth (bar amplitudes are thought to scale with depth). These bedforms were not bedload sheets (Whiting et al., 1988; Nelson et al., 2009) because they did not display strong sorting and their amplitudes were much larger than the 1–2 times D_{84} characteristic of low-amplitude sheets. These features were probably not dunes, given their regular alternating pattern.

No present theory for alternate bar instability is likely to predict the occurrence of bars for our experimental conditions. One of the classical problems of theoretical morphodynamics is the development of alternate bars in a straight channel from an initially flat bed. Analytical linear stability analyses, in which the growth or damping of small perturbations of the bed is mathematically predicted as a function of the perturbation wavenumber and flow conditions, have been used to understand the mechanisms of bar formation, the connection between alternate bars and river meandering, and the conditions necessary for bar formation (e.g., Ikeda et al., 1981; Blondeaux and Seminara, 1985; Colombini et al., 1987; Nelson, 1990). In general, these analyses find that the width-to-depth ratio β must be above a threshold value β_c, which usually ranges from around 12–15, and the most unstable wavelength is typically around 6 channel widths (Seminara, 2010). These theories assume that sediment is transported at the channel's transport capacity, which was the case in our experiments.

The width-to-depth ratio in our experiments β was about 8, which is much lower than theory would predict is necessary for bars to form from an initially flat bed. Additionally, the characteristic wavelength of the bars in our experiments was only about 3 times the channel width, much shorter than theory would predict. So we are faced with the question: Why did alternate bars develop in our experiments when theory predicts that the flow was too deep to allow them to form?

Most alternate bar stability analyses model the hydrodynamics with the shallow-water equations because for typical bar scales the ratio of the water depth to the bar wavelength is small. Additionally, Tubino et al. (1999) performed a linear stability analysis of alternate bars using a three-dimensional flow model and found stability conditions that were very similar to those found using a depth-averaged model, suggesting that the matter of which level of hydrodynamic complexity to include in bar stability analyses is fairly settled (Seminara, 2010). However, Furbish (1998), in an attempt to understand bedforms in steep mountain streams, noted that certain velocity correlation terms that are neglected for smooth alluvial channels can be a significant part of the momentum balance of steep channels. He performed a linear stability analysis retaining the streamwise correlation terms and found that in certain conditions his model predicted critical width-to-depth ratios for bar instability that were much smaller than the critical ratios that are predicted when correlation terms are neglected; in some cases, his model predicted $\beta_c < 5$.

We have used the Furbish (1998) model to calculate a stability curve for alternate bar formation for the conditions of our experiment, and the model predicts a minimum β_c of about 15 (Fig. 7), so the Furbish (1998) model still would not predict bars to form in our experiment. However, we suspect that a three-dimensional analysis incorporating Reynolds stress terms neglected in the Tubino et al. (1999) analysis may reveal a heretofore unrecognized alternate bar instability that could explain our experimental observations. Recent work on tidal dunes and bars (Blondeaux and Vittori, 2011) used a three-dimensional hydrodynamic model to uncover two modes of instability: one associated with long-wavelength dunes, and one associated with shorter-wavelength tidal alternate bars. The tidal alternate bar instability cannot be predicted using a depth-averaged approach, and their prediction has been shown to correspond with experimental observations by Tambroni et al. (2005). Perhaps a similar analysis for fluvial bars could explain our experimental observations.

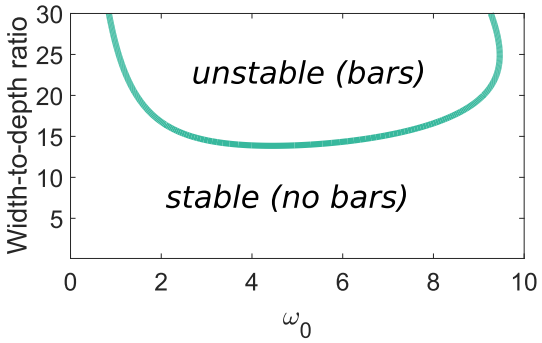

Fig. 7. Stability diagram for alternate bars for our experimental conditions using the model of Furbish (1998). The horizontal axis (ω_0) is the dimensionless wavenumber of the perturbation.

Our experiments are not the only ones to have developed alternate bars with low width-to-depth ratios. Wilkinson et al. (2008) reported the development of alternate bars in flume experiments using a fine gravel mixture with width-to-depth ratios as low as 3.8. They were unable, however, to measure bar migration rates, and most of their experiments were at or above critical flow conditions.

5. Conclusions

We conducted a flume experiment to explore how unsteady flow and changing sediment supply influence the morphodynamic evolution of gravel-bed rivers. At the scale of the entire flume, we found that unsteady flow had very little effect on equilibrium channel conditions, potentially because the flow variations were able to be accommodated entirely by the rate and size distribution of the bedload transport. Increasing the sediment supply caused the bed and water surface slopes to increase considerably.

The relative effects of unsteady flows and increased sediment supply were much different at the scale of gravel bedforms. During our experiment, downstream migrating bedforms strongly resembling alternate bars developed. The migration speed of these bars when subject to repeated hydrographs was much slower than the migration speed under steady flow, suggesting that temporary increases and decreases in sediment transport rates resulting from unsteady flow were primarily reflected by increases and decreases in bar amplitude but not migration.

Analytical linear stability analyses for alternate bar formation would not have predicted the development of bars in our experiment, primarily because the width-to-depth ratio was too low. However, the presence of bars in our experiment, and in other experiments conducted with low width-to-depth ratios, suggests an opportunity to revisit bar theory to potentially reveal new mechanisms of bar formation.

Acknowledgments

We would like to thank Aaron Schoelkopf for his assistance with the experiments and bedform data collection. Ideas in this paper were improved through conversations with Marco Redolfi, Bill Dietrich, and Elowyn Yager. Comments from two anonymous reviewers, the associate editor, and the editor improved the clarity of the manuscript. This work was funded by the U.S. National Science Foundation grant EAR-1425067.

References

Bankert, A.R., Nelson, P.A., 2017. Alternate bar dynamics in response to increases and decreases of sediment supply. Sedimentology 65, 702–720. https://doi.org/10.1111/sed.12399.

Blondeaux, P., Seminara, G., 1985. A unified bar-bend theory of river meanders. J. Fluid Mech. 157, 449–470.

Blondeaux, P., Vittori, G., 2011. Dunes and alternate bars in tidal channels. J. Fluid Mech. 670, 558–580.

Brayshaw, A.C., Frostick, L.E., Reid, I., 1983. The hydrodynamics of particle clusters and sediment entrapment in coarse alluvial channels. Sedimentology 30, 137–143.

Brew, A.K., Morgan, J.A., Nelson, P.A., 2015. Bankfull width controls on riffle-pool morphology under conditions of increased sediment supply: field observations during the Elwha River dam removal project. Proceedings of the 3rd Joint Federal Interagency Conference on Sedimentation and Hydrologic Modeling, April 19-23, 2015, Reno, Nevada, USA. pp. 1633–1643.

Carling, P.A., 1999. Subaqueous gravel dunes. J. Sediment. Res. 69, 534–545.

Carling, P.A., Orr, H.G., 2000. Morphology of riffle-pool sequences in the River Severn, England. Earth Surf. Process. Landf. 25, 369–384.

Colombini, M., Seminara, G., Tubino, M., 1987. Finite-amplitude alternate bars. J. Fluid Mech. 181, 213–232.

Dietrich, W.E., Kirchner, J.W., Ikeda, H., Iseya, F., 1989. Sediment supply and the development of the coarse surface layer in gravel-bedded rivers. Nature 340, 215–217.

Furbish, D.J., 1998. Irregular bed forms in steep, rough channels 1. Stability analysis. Water Resour. Res. 34, 3635–3648.

Hassan, M.A., Church, M., 2001. Sensitivity of bed load transport in Harris Creek: seasonal and spatial variation over a cobble-gravel bar. Water Resour. Res. 37, 813–825. https://doi.org/10.1029/2000WR900346.

Humphries, R., Venditti, J.G., Sklar, L.S., Wooster, J.K., 2012. Experimental evidence for the effect of hydrographs on sediment pulse dynamics in gravel-bedded rivers. Water Resour. Res. 48, https://doi.org/10.1029/2011WR010419.

Ikeda, S., Parker, G., Sawai, K., 1981. Bend theory of river meanders. Part 1. Linear development. J. Fluid Mech. 112, 363–377.

Lane, E.W., 1955. The importance of fluvial geomorphology in hydraulic engineering. Am. Soc. Civ. Eng. Proc. Separate 81, 1–17.

Lanzoni, S., 2000a. Experiments on bar formation in a straight flume. 1. Uniform sediment. Water Resour. Res. 36, 3337–3350.

Lanzoni, S., 2000b. Experiments on bar formation in a straight flume. 2. Graded sediment. Water Resour. Res. 36, 3351–3364.

Lisle, T.E., Hilton, S., 1992. Volume of fine sediment in pools: an index of sediment supply in gravel-bed streams. Water Resour. Bull. 28, 371–383.

Mao, L., 2012. The effect of hydrographs on bed load transport and bed sediment spatial arrangement. J. Geophys. Res. 117, https://doi.org/10.1029/2012JF002428.

Martin, R.L., Jerolmack, D.J., 2013. Origin of hysteresis in bed form response to unsteady flows: bed form hysteresis in unsteady flows. Water Resour. Res. 49, 1314–1333. https://doi.org/10.1002/wrcr.20093.

Milan, D.J., 2013. Sediment routing hypothesis for pool-riffle maintenance. Earth Surf. Process. Landf. 38, 1623–1641. https://doi.org/10.1002/esp.3395.

Montgomery, D.R., Buffington, J.M., 1997. Channel-reach morphology in mountain drainage basins. Bull. Geol. Soc. Am. 109, 596–611.

Morgan, J.A., 2018. The Effects of Sediment Supply, Width Variations, and Unsteady Flow on Riffle-Pool Dynamics.Ph.D. thesis. Colorado State University, Fort Collins, CO.

Morgan, J.A., Brogan, D.J., Nelson, P.A., 2017. Application of structure-from-motion photogrammetry in laboratory flumes. Geomorphology 276, 125–143.

Nelson, J.M., 1990. The initial instability and finite-amplitude stability of alternate bars in straight channels. Earth Sci. Rev. 29, 97–115.

Nelson, P.A., Bolla Pittaluga, M., Seminara, G., 2014. Finite amplitude bars in mixed bedrock-alluvial channels. J. Geophys. Res. Earth Surf. 119, 566–587. https://doi.org/10.1002/2013JF002957.

Nelson, P.A., Venditti, J.G., Dietrich, W.E., Kirchner, J.W., Ikeda, H., Iseya, F., Sklar, L.S., 2009. Response of bed surface patchiness to reductions in sediment supply. J. Geophys. Res. 114, https://doi.org/10.1029/2008JF001144. F02005.

Parker, G., 2008. Transport of gravel and sediment mixtures. In: Garcia, M.H., Parker, G. (Eds.), Sedimentation Engineering, ASCE Manual No. 110. American Society of Civil Engineers, Reston, VA, pp. 165–252.

Parker, G., Hassan, M., Wilcock, P., 2008. Adjustment of the bed surface size distribution of gravel-bed rivers in response to cycled hydrographs. In: Habersack, H., Piegay, H., Rinaldi, M. (Eds.), Gravel Bed Rivers VI: From Process Understanding to River Restoration. Elsevier., pp. 241–285.

Parker, G., Toro-Escobar, C.M., Ramey, M., Beck, S., 2003. Effect of floodwater extraction on mountain stream morphology. J. Hydraul. Eng. 129, 885. https://doi.org/10.1061/(ASCE)0733-9429(2003)129:11(885).

Podolak, C.J.P., Wilcock, P.R., 2013. Experimental study of the response of a gravel streambed to increased sediment supply. Earth Surf. Process. Landf. 38, 1748–1764. https://doi.org/10.1002/esp.3468.

Recking, A., Leduc, P., Liébault, F., Church, M., 2012. A field investigation of the influence of sediment supply on step-pool morphology and stability. Geomorphology 139-140, 53–66. https://doi.org/10.1016/j.geomorph.2011.09.024.

Richards, K.S., 1976. Channel width and the riffle-pool sequence. Geol. Soc. Am. Bull. 87, 883–890.

Seminara, G., 2010. Fluvial sedimentary patterns. Annu. Rev. Fluid Mech. 42, 43–66. https://doi.org/10.1146/annurev-fluid-121108-145612.

Tambroni, N., Pittaluga, M.B., Seminara, G., 2005. Laboratory observations of the morphodynamic evolution of tidal channels and tidal inlets. J. Geophys. Res. 110, https://doi.org/10.1029/2004JF000243. F04009.

Tubino, M., 1991a. Flume experiments on alternate bars in unsteady flow. Fluvial hydraulics of mountain regions. In: Armanini, Aronne, Silvio, Giampaolo Di (Eds.), Lecture Notes in Earth Sciences. 37. pp. 103–117.

Tubino, M., 1991b. Growth of alternate bars in unsteady flow. Water Resour. Res. 27, 37–52.

Tubino, M., Repetto, R., Zolezzi, G., 1999. Free bars in rivers. J. Hydraul. Res. 37, 759–775.

van der Mark, C.F., Blom, A., Hulscher, S.J.M.H., 2008. Quantification of variability in bedform geometry. J. Geophys. Res. 113, https://doi.org/10.1029/2007JF000940.

Venditti, J.G., Nelson, P.A., Bradley, R.W., Haught, D., Gitto, A.B., 2017. Bedforms, structures, patches, and sediment supply in Gravel-Bed Rivers. Gravel-Bed Rivers: Process and Disasters. pp. 439–466.

Venditti, J.G., Nelson, P.A., Minear, J.T., Wooster, J., Dietrich, W.E., 2012. Alternate bar response to sediment supply termination. J. Geophys. Res. https://doi.org/10.1029/2011JF002254.

Whiting, P.J., Dietrich, W.E., Leopold, L.B., Drake, T.G., Shreve, R.L., 1988. Bedload sheets in heterogeneous sediment. Geology 16, 105–108.

Wilcock, P.R., Crowe, J.C., 2003. Surface-based transport model for mixed-size sediment. J. Hydraul. Eng. 129, 120–128. https://doi.org/10.1061/(ASCE)0733-9429(2003)129:2(120).

Wilcock, P.R., McArdell, B.W., 1993. Surface-based fractional transport rates: mobilization thresholds and partial transport of a sand-gravel sediment. Water Resour. Res. 29, 1297–1312.

Wilkinson, S.N., Rutherfurd, I.D., Keller, R.J., 2008. An experimental test of whether bar instability contributes to the formation, periodicity and maintenance of pool-riffle sequences. Earth Surf. Process. Landf. 33, 1742–1756. https://doi.org/10.1002/esp.1645.

Wong, M., Parker, G., 2006. One-dimensional modeling of bed evolution in a gravel bed river subject to a cycled flood hydrograph. J. Geophys. Res. 111, https://doi.org/10.1029/2006JF000478. F03018.